Experimental energy straggling of protons in SiO_2

J. H. R. dos Santos, P. L. Grande, M. Behar, and J. F. Dias
Instituto de Física da Universidade Federal do Rio Grande do Sul, Avenida Bento Goncalves 9500, 91501-970, Porto Alegre, Rio Grande do Sul, Brazil

N. R. Arista, J. C. Eckardt, and G. H. Lantschner
Centro Atómico Bariloche, Comisión Nacional de Energía Atómica, RA-8400 San Carlos de Bariloche, Argentina
(Received 7 May 2003; published 23 October 2003)

The energy straggling of proton beams in SiO_2 has been measured in the energy range from 30 to 1500 keV using the transmission, nuclear reaction analysis and Rutherford backscattering techniques. The experimental results are compared with theoretical models. We observe that at energies around 200 keV the values obtained are larger than theoretical estimations. The straggling effect produced by the electron bunching in molecular media was calculated and it was found to be a possible cause of these differences at intermediate energies.

DOI: 10.1103/PhysRevA.68.042903 PACS number(s): 34.50.Bw

I. INTRODUCTION

The slowing down of fast light ions in matter is mainly due to interactions with the target material electrons. Due to the different energy transfers involved, and the dispersion in the number of interactions, the energy loss experienced by an ion-beam traversing matter is a statistical process which leads to an energy straggling in the case of pure elements as well as compound materials. The energy broadening of the ion beams arising from this phenomenon has technological implications such as the spatial dispersion of implantation profiles. Usually the energy straggling is characterized by the mean square deviation Ω^2 of the energy distributions.

At low energies only the valence electrons participate in the energy loss and straggling while at higher ion velocities the atomic core electrons also contribute [1,2]. This means that when considering compound materials the energy straggling is affected by chemical bounds at low energies. Due to the fact that the straggling Ω^2 is essentially determined by the processes of larger energy transfer, at higher energies the chemical bound effect plays a minor role due to the increasing participation of atomic core electrons. In this case a first-order approximation to Ω^2 can be calculated by adding the Ω_j^2 values of the composing elements considering the stoichiometric proportions. That is the so-called *additivity rule*.

In an earlier paper Bohr [3] gave a simple expression for Ω^2 of single elements valid at high energies where all the target electrons contribute to the energy loss

$$\Omega_B^2 = 4\pi Z_1^2 e^4 Z_2 N \langle x \rangle, \tag{1}$$

where Z_1 and Z_2 are the projectile and target atomic numbers, respectively, N is the target atomic density and $\langle x \rangle$ is its thickness. This Bohr value is frequently used as a reference value. It can also be calculated for compound materials through the additivity rule.

In this paper we present energy straggling measurements and calculations for proton beams in SiO_2, a compound material of great technological interest for which almost no data are available. The experimental determinations cover the energy range from 30 to 1500 keV and has been performed employing different experimental techniques. A comparison with recent theoretical predictions for oxides [4] is included as well with other theoretical values [5] obtained through the additivity rule.

When considering metals or more generally conductors, the literature shows a great effort in studying the ion-beam energy loss ΔE, while the energy straggling is investigated in a lesser extent because of experimental difficulties. In the case of insulators the measurements are even more troublesome, and therefore scarce.

Compared with the energy-loss experiments, the determination of the energy straggling sets more severe requirements to the spectrometric methods and the target preparation. For the two most widespread experimental methods, i.e., the transmission and the backscattering methods, the targets must be as smooth and as homogeneous as possible, since target inhomogeneities and roughness introduce an important additional energy straggling. In the case of insulators provisions have to be made in order to avoid target charge buildup effects, or at least keep them within negligible limits.

In the following sections the experimental methods are described, the results are discussed, and followed by theoretical considerations.

II. EXPERIMENTAL PROCEDURE

The present straggling determinations were made employing the transmission method at lower and intermediate energies at the Centro Atómico Bariloche's (CAB) Atomic Collisions laboratory (30–200 keV), and the nuclear reaction analysis (NRA) and Rutherford backscattering (RBS) techniques between 150 and 1500 keV at the Instituto de Física of the Universidade Federal do Rio Grande do Sul (IF-UFRGS) laboratory.

A. Transmission experiments

The self-supported foils used in the transmission measurements were made by evaporation under clean vacuum conditions on a very smooth plastic substrate [6], which was subsequently dissolved to a limit to make eventual residues undetectable in energy-loss experiments. The mean foil thicknesses $\langle x \rangle$ were 12.2 nm and have been determined by

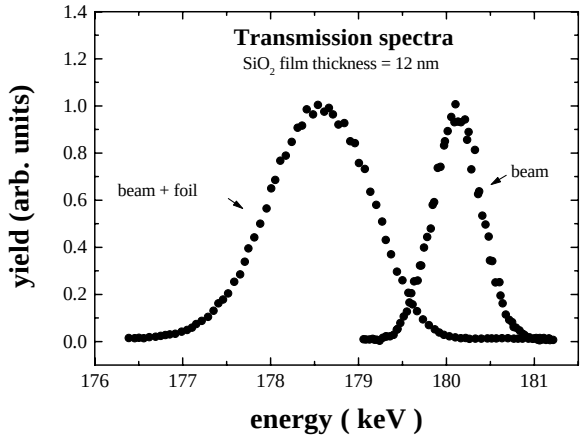

FIG. 1. Energy spectra of a 180.12 keV proton beam before and after traversing a 12 nm SiO_2 foil.

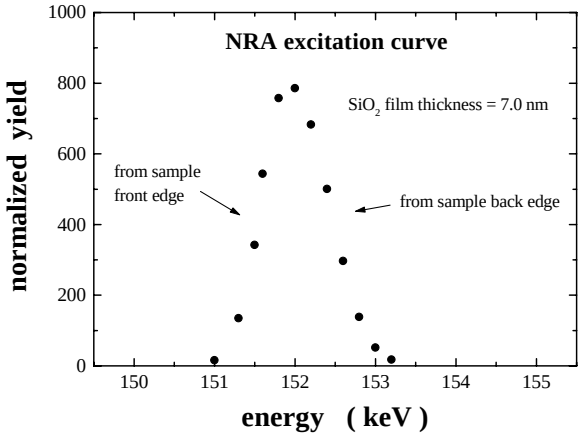

FIG. 2. Nuclear-reaction analysis spectrum corresponding to the $^{18}O(p,\alpha)^{15}N$ reaction ($E_r = 151$ keV) using a 7 nm $Si^{18}O_2$ target.

energy-loss measurements and comparison with 200 keV stopping-power values from Ref. [7]. To characterize their inhomogeneity we employed an ion-beam analysis using H^+ and He^+ beams [8], which allows the determination of an upper bound for the standard deviation σ of the foil thickness distribution. The resulting upper bounds for the roughness coefficient $\rho = \sigma/\langle x \rangle$ ranged from 10 to 14%. This *in situ* analysis has been compared with atomic force microscope studies in previous measurements showing small differences.

The proton beam for the transmission method was generated by electrostatic acceleration of ions produced in a rf ion source. Electrostatic focusing, magnetic mass selection stages, and collimation defined the final beam. Up to ten foils were mounted on a movable holder which allowed changing the targets and removing them from the beam path during the operation of the accelerator. The energy analysis was performed by an electrostatic analyzer with 0.3% (full width at half maximum—FWHM) resolution, positioned in the forward beam direction. The particles were detected by a discrete dynode electron multiplier followed by a conventional pulse counting electronics. Spectra were recorded by a multichannel scaler with channels switched synchronously with the energy analyzer plate potential.

Foil thickening of the self-supporting foils by beam bombardment [9] was held within negligible limits by using a low ion current density of $\sim 10^{-9}$ A/cm^2, and irradiation times of less than 2 min per spectrum. In this way no change in foil characteristics could be detected during the time of measurements.

Target charging up was avoided by introducing a low-energy electron shower in the target chamber. At the energies of this experiment and with the employed foil thicknesses, the transmission experiment spectra were nearly Gaussian. A typical spectrum is shown in Fig. 1. This made it possible to obtain the Ω values determining the FWHM from the measured spectra and dividing them by the conventional $\sqrt{8 \ln 2} = 2.355$ factor for conversion to standard deviations. The precision of the straggling determinations is ~ 50 eV.

B. NRA and RBS experiments

For both types of experiments, the samples were prepared at the IF-UFRGS by thermal oxidation of Si wafers in an O_2 atmosphere. Transmission Electron Microscopy revealed the films roughnesses to be less than 0.4 nm.

At 151 keV, the measurement of proton straggling in SiO_2 was carried out by Nuclear Reaction Analysis (NRA) through the $^{18}O(p,\alpha)^{15}N$ resonant reaction at 151.2 keV. This reaction has one of the narrowest resonances ($\Gamma = 50$ eV) among the resonant charged particle nuclear reactions, which implies an excellent depth resolution. In order to obtain the excitation curve corresponding to the SiO_2 film, we have changed the energy of the impinging proton beam and detected, under similar conditions, the alpha particles product of the nuclear reaction. In this way, one is able to determine the excitation curve corresponding to the film as a function of the projectile energy by comparing the actual beam energy with the one corresponding to the resonance. Once the excitation curve was completed, we transformed the energy scale into depth scale by using the well-known stopping power of protons in SiO_2, in this way, it is possible to determine the thickness of the SiO_2 film.

The ion beam was provided by the 500 kV ion implanter of the Instituto de Física, Universidade Federal Rio Grande do Sul, Brazil. The α particles emitted in the reaction were detected by a large Si surface barrier detector (600 mm^2) placed at 30 mm from the target.

In Fig. 2, we display the excitation curve obtained using protons from a 7.0 nm-$Si^{18}O_2$ film. The apparent straggling that would be extracted out of the excitation curve comprises: (a) the width of the nuclear resonance ($\Gamma = 50$ eV); (b) the Doppler broadening caused by atomic vibrations in the target; (c) the energy spread of the analyzing beam; and, (d) the energy straggling. We have fitted the excitation curves with an algorithm that performs a numerical convolution of the above distributions and leaves the energy straggling as a free parameter. The probability distributions associated with effects (b), (c), and (d) were assumed to be normal whereas the one connected with (a) is a Lorentzian. The contributions of the effects (a), (b), and (c) to the NRA spectra were experimentally determined by measuring the front edge of a thick $Si^{18}O_2$ film. The edge width results of the convolution of the resonance width, the Doppler broadening, and the en-

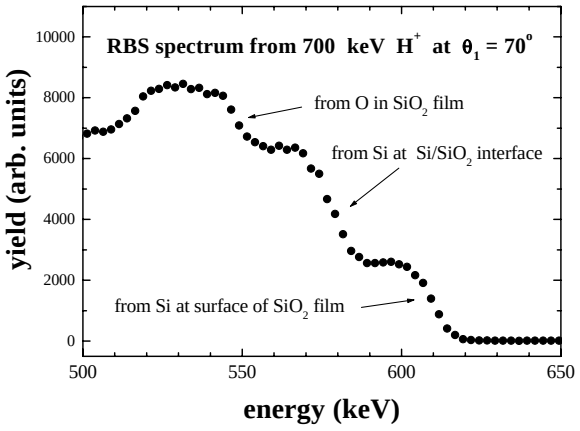

FIG. 3. Typical spectrum of a 170° Rutherford backscattering measurement from SiO_2 oxidized on a Si-wafer tilted 70° with respect to the proton beam.

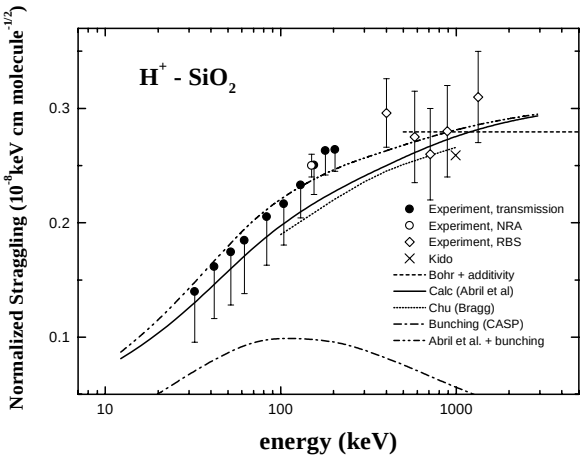

FIG. 4. Experimental normalized energy straggling $s(E)$ data points together with theoretical calculations and estimations. Solid circles, transmission experiments; open circle, NRA value; diamonds, RBS experiments; cross, experimental value from Ref. [14]; solid line, dielectric function calculations [4]; dotted line, theoretical values based on Ref. [5]; dashed line, asymptotic limit derived from Bohr formula; dot-dashed line, calculated bunching effect contribution; dash-double-dotted, dielectric function calculation plus bunching effect.

ergy spread of the analyzing beam were used as input in the fitting algorithm.

At higher energies (above 400 keV), the well-known Rutherford backscattering technique was employed. The incident protons backscattered by the SiO_2 film were detected by a Si barrier detector of 7 keV electronic resolution placed at an angle of 170° with respect to the incident beam. The thickness of the targets were determined by measuring the energy loss suffered by the projectile in its trajectory before and after the backscattering process has occurred. Furthermore, by using the H stopping power in SiO_2 it is possible to transform the energy into depth scale, which allows the determination of the thickness of the film. In the present case we have used the stopping-power values from the SRIM program [10] whose values agree within 2% with those of Ref. [7] employed in the transmission experiments. The targets were tilted at angles between 30° and 70° in order to improve the depth resolution of the experiments. The thicknesses determined in this way were 96 nm and 194 nm, respectively, with typical errors of the order of 5%. The ion beams were provided by the 500 kV ion implanter and the 3 MV tandem accelerator of the Instituto de Física, Universidade Federal Rio Grande do Sul, Brazil.

Figure 3 shows a spectrum obtained for 700 keV protons backscattered from a sample with a SiO_2 film of 96 nm oxidized on a Si wafer, tilted at an angle of 70° with respect to the beam direction. Going from higher to lower energies, three steps are seen: the first one, around 610 keV, is due to protons backscattered from Si atoms at the SiO_2 surface. The second step, around 578 keV, corresponds to protons backscattered from Si atoms at the SiO_2-Si interface. Finally, the hump on top of the spectrum comes from protons backscattered from the O atoms of the SiO_2 film. As can be observed, the width of the edge corresponding to the backscattering of protons by Si atoms at the Si/SiO_2 interface (rear edge) is larger than the width of the edge determined by protons backscattered by Si atoms at the surface (front edge). The rear-edge width is the result of the convolution of the energy straggling, detector resolution, beam spread, geometrical broadening due to the finite detector acceptance angle, and multiple-scattering contributions, whereas the front-edge width is due to the system detector resolution, beam spread, and partial geometrical factors. In order to obtain the total-energy straggling Ω_t^2 in the SiO_2 film, we fitted both edges to error functions and afterwards deconvoluted the width of the front edge from the one of the rear edge. In this way the detector resolution and beam spread were subtracted. In doing so we assumed that the involved distributions follow normal statistics. The geometrical broadening due to the detector acceptance (4 deg) and the multiple-scattering effect was subtracted following the procedure of Ref. [11].

Because of the energy loss in the backscattering collision, the variance Ω_t^2 corresponding to the energy straggling is given by [12]

$$\Omega_t^2 = K^2 s_{in}^2 N \frac{\langle x \rangle}{\cos\theta_1} + s_{out}^2 N \frac{\langle x \rangle}{\cos\theta_2}, \tag{2}$$

where N is the SiO_2 density of the target, $\langle x \rangle$ is the SiO_2 film thickness, $s_{in}^2 N(\langle x \rangle/\cos\theta_1)$ and $s_{out}^2 N(\langle x \rangle \cos\theta_2)$ are the variances associated with the inward and outward paths, respectively, and K is the kinematic factor for backscattering of protons by Si. Owing to the relatively large kinematic factor ($K=0.8668$), we may take $s_{in}=s_{out}\equiv s(\overline{E})$, where $\overline{E}$ is the mean value between the energies before and after the collision at the interface.

The CAB and the IF-UFRGS results for $s(E)$ are presented in Fig. 4 and will be discussed in the following section.

III. RESULTS

The complete set of results measured at CAB and IF-UFRGS are shown in Fig. 4. The measurements at CAB range from 30 to 200 keV. As can be observed there is quite a good agreement between the transmission and NRA results

for 150 keV. On the other hand the RBS measurements cover the upper range of the present measurements going between 400 and 1500 keV. In the same figure several other straggling estimations and calculations are shown: (a) the values resulting from Bohr's high-energy formula [3] using the additivity rule and the separate Si and O straggling values, (b) previous calculations by Chu [5] combined also according to the additivity rule, and (c) recent calculations by Abril *et al.* [4] based on Mermin fittings of dielectric functions. One can observe that at energies above $\sim$100 keV, in the region around 200 keV the experimental values are somewhat higher than these theoretical predictions. Possible explanations of this difference will be discussed below.

The present experimental data up to 200 keV data are corrected for the foil roughness using the formula $\Omega^2 = \Omega^2_{\mathrm{exp}} - \rho^2 \Delta E^2$ [13], where Ω_{exp} is the measured straggling and $\rho = \sigma / \langle x \rangle$ is the ratio of the standard deviation σ of the foil thickness relative to its mean thickness $\langle x \rangle$. As mentioned before in place of ρ we used upper bound values for this standard deviation determined by an *in situ* beam-foil method [8]. In doing so, some overcorrection of the data may arise. These values of the corrections were depicted in form of asymmetric error bars whose lengths are determined by the upper bounds to the ρ coefficients. The combined energy spread due to spectrometer resolution and the beam energy spread were separately determined for each energy and subtracted from the measured Ω^2 values leading to the experimental straggling Ω^2_{exp}. In this range the roughness effect is more important than the statistical errors.

At the higher energies corresponding to the IF-UFRGS measurements the influence of the roughness effect is smaller, and the error bars in the data points represent the statistical errors. One can observe the dominating role of the target roughness effect at the low-energy range, whereas towards higher energies the contribution of the energy straggling inherent to the energy-loss process increases over that due to the roughness effect, becoming dominant at the upper range covered in this work.

The only previously published experimental data point [14] is also included in the figure. In comparing the values shown in this figure we observe a good agreement with the theoretical predictions in the low-energy range up to $\sim$100 keV. However, differences beyond the experimental error bars are observed at higher energies.

In the following section we analyze the effect of target electron density bunching as a possible reason for these discrepancies. The result of the calculations are depicted in Fig. 4, showing the isolated bunching contribution (dotted line) as well as the convolution with dielectric function calculations of Abril et al. [4]. As can be seen the bunching effect is expected to be largest at energies around 100 keV, and decreases towards higher energies. Therefore it seems to be a possible cause of the observed discrepancies.

IV. THEORETICAL CONSIDERATIONS: THE BUNCHING EFFECT

The experimental results for the energy straggling at low energies show a reasonably good agreement with the theoretical estimations. However, we find discrepancies with the theoretical values at intermediate energies. We have searched possible causes to explain these differences. One possible source of additional straggling is the effect of charge state fluctuation. This effect is expected to be more important for energies around the stopping-power maximum (i.e., somewhat below the region of the largest observed discrepancies). Additionally, previous estimations by Besenbacher *et al.* [13] indicate that the effect of charge state fluctuation on the energy straggling are expected to be negligible for protons in solids.

A further effect that we considered is the momentum distribution of the inner-shell electrons. This yields a correction to the energy straggling, as predicted by the Bethe-Livingston theory [15], which produces an enhancement at high energies of the form

$$\Omega^2 \simeq \Omega_B^2 \left[1 + \frac{4}{3} \frac{\langle K \rangle}{mv^2} \ln\left(\frac{2mv^2}{I_i} \right) \right], \tag{3}$$

where $\langle K \rangle$ is the average kinetic energy of target electrons and I_i is a mean excitation energy. This effect is predicted both for inner shells [15,16], as well as for valence electrons [17].

However, we note that this effect is included in the comprehensive theoretical calculations in Ref. [4], and that it produces a slight enhancement of the straggling in the high-energy region (beyond 1 MeV). The behavior of the experimental points at high energies appear to be consistent with a small enhancement effect predicted by the Bethe-Livingston model.

We considered here another possible contribution to the energy straggling coming from the so-called bunching effect, which is produced by the inhomogeneous distribution of the atomic target electrons participating in the energy-loss process. Indeed, this is due to the fact that all the electrons are grouped in shells bound to the target nuclei (this correction would vanish if all the electrons were distributed uniformly throughout the target). It has been shown in previous papers that this introduces an additional source of energy-loss fluctuation, which is similar to the effect produced by foil roughness or target inhomogeneities [13,18].

The bunching effect was taken into account according to the formulation developed by Sigmund [19] extended to all subshells of Si and O atoms. A detailed description of the calculation is given in the Appendix. Here basically the same notation as in Ref. [19] will be used. In this calculation we take into account the impact-parameter dependence of the energy loss through the function $Q_i(b)$, for each target atom in the SiO_2 molecules (and where b is the impact parameter), so that the stopping cross section S may be represented by $S = \int d^2b \Sigma_i Q_i(b)$. As shown in the Appendix, the energy straggling may be decomposed into intra-atomic and inter-atomic contributions as follows,

$$\Delta W = \Delta W_{intra} + \Delta W_{inter}, \tag{4}$$

where the values of ΔW_{intra} and ΔW_{inter} are given by Eqs. (A13) and (A14) in the Appendix.

We have evaluated both contributions using the CASP model [20] to calculate the $Q_i(b)$ values for both Si and O components of SiO_2 (see the Appendix for details). We found that the dominating term is by far the intra-atomic bunching ΔW_{intra} (yielding more than 90% of the correction).

As mentioned before, the magnitude of this effect appears to be in reasonable agreement with the experiment at intermediate energies.

V. CONCLUDING REMARKS

We have performed energy straggling measurements of protons in SiO_2 in an extended energy range going from 30 keV to 1.5 MeV making use of a combination of experimental techniques: transmission energy-loss method, nuclear reaction analysis, and Rutherford backscattering. The results obtained from these various techniques are in consistent agreement.

Additionally, the results show the following features.

(a) A good agreement with published calculations by Abril *et al.* [4] can be observed at energies up to ~ 100 keV.

(b) At intermediate energies the experiment yield higher values than the theoretical curves.

(c) We discuss the possible reason for these discrepancies considering the influence of various mechanisms (charge exchange, inner-shell corrections, and bunching effect).

(d) We calculate the bunching effect and find it to be important in the intermediate energy region, therefore being the most likely origin of the observed discrepancies.

Based on these results, we estimate that similar effects may be expected to arise in other elements with many shells. A systematic study of energy straggling in various other compound materials may be useful to elucidate the mechanism of electron bunching as a relevant mechanism for the difference between oxides and pure elements.

ACKNOWLEDGMENTS

We would like to thank Professor H. Boudinov for preparing the SiO_2 films used in the RBS experiments. This work was partially supported by the Argentine Agencia Nacional de Promoción Científica y Tecnológica, Project No. PICT 03-03579, the Consejo Nacional de Investigaciones Científicas y Técnicas (PIP 4267/96), the IAEA Contract No. 11313/RO, and the Cooperation Program SETCIP-CAPES 33/02 (BR/A - U111/008).

APPENDIX: THE BUNCHING EFFECT

The current estimation of the bunching effect for SiO_2 follows the lines of formulation given in Ref. [19].

Let us consider a solid target with z atoms (the extension for different atoms as in SiO_2 will be straightforward) in a piece of volume penetrated by the ion beam. The atoms are labeled by Greek indices and the electrons in each subshell by italic ones. The atoms are then located at $\vec{r}_\alpha$ with lateral component given by $\vec{\rho}_\alpha$. Assuming a straight-line trajectory defined by an impact parameter $\vec{b}$, the energy loss in a given trajectory is given by

$$\Delta E = \sum_{\alpha,i} \Delta\varepsilon_i(\vec{b}-\vec{\rho}_\alpha). \tag{A1}$$

Here $\Delta\varepsilon_i$ is the fluctuating energy loss due to ionization/excitation of the ith electron and it is distributed according to its quantum-mechanical probability. Therefore, it has to be distinguished from $Q_i(b)$ that its mean value

$$Q_i(b) = \langle \Delta\varepsilon_i \rangle_{QM}. \tag{A2}$$

The average energy loss is found by taking the quantum-mechanical average as well as by randomizing the point of impact

$$\langle \Delta E \rangle = \frac{1}{A}\int d^2b \sum_{\alpha,i} Q_i(\vec{b}-\vec{\rho}_\alpha), \tag{A3}$$

where A is the cross-sectional area of the beam. If this area is large so that the integration is extended over the infinite traversal plane $\vec{b}$, we will have

$$\langle \Delta E \rangle = \frac{1}{A}\sum_\alpha \int d^2b \sum_i Q_i(b) = \frac{z}{A}S = NxS, \tag{A4}$$

where S is the stopping cross section, $S=\int d^2b \Sigma_i Q_i(b)$, and $z=NxA$. Thus, no bunching effect is found for the mean-energy loss (within the approximation that the energy loss $\Delta\varepsilon_i$ is not affected by the neighborhood).

On the other hand, the mean-square energy loss reads

$$\langle \Delta E^2 \rangle = \frac{1}{A}\int d^2b \sum_{\alpha,i} \langle \Delta\varepsilon_i^2 \rangle_{QM}(\vec{b}-\vec{\rho}_\alpha) + \frac{1}{A}\int d^2b \sum_{(\alpha,i)\neq(\beta,j)} Q_i(\vec{b}-\vec{\rho}_\alpha) Q_j(\vec{b}-\vec{\rho}_\beta). \tag{A5}$$

We can replace the integration variable $\vec{b}$ by $\vec{b}+\vec{\rho}_\alpha$ in each individual term. This yields

$$\langle \Delta E^2 \rangle = \frac{z}{A}W + \frac{z}{A}{\sum_{\beta,i,j}}' \int d^2b \;\; Q_i(\vec{b}) Q_j(\vec{b}-\vec{\rho}_\beta). \tag{A6}$$

The apostrophe indicates omission of the vector pointing from one target nucleus on itself for the case of $i=j$. W is the usual (uncorrelated) straggling parameter,

$$W = \int d^2b \sum_i \langle \Delta\varepsilon_i^2 \rangle_{QM}(\vec{b}). \tag{A7}$$

The total energy loss straggling [using Eq. (A3) and (A6)] will be given by

$$\langle \Delta E^2 \rangle - \langle \Delta E \rangle^2 = \frac{z}{A}W + \frac{z}{A}{\sum_{\beta,i,j}}' \int d^2b \;\; Q_i(\vec{b}) Q_j(\vec{b}-\vec{\rho}_\beta) - \frac{z}{A}\int d^2b \sum_i Q_i(b) \;\; \frac{z}{A}\int d^2b \sum_j Q_j(b). \tag{A8}$$

The last two terms are related to the bunching effect ΔW

$$\Delta W = \frac{z}{A} \sum_i \int d^2b Q_i(\vec{b}) \times \sum_j \left(\sum_\beta{}' Q_j(\vec{b} - \vec{\rho}_\beta) - \frac{z}{A} \int d^2b Q_j(b) \right), \tag{A9}$$

which can be divided in intra-atomic and interatomic bunching as

$$\Delta W = \Delta W_{intra} + \Delta W_{inter}, \tag{A10}$$

with

$$\Delta W_{intra} = Nx \sum_i \int d^2b Q_i(\vec{b}) \sum_{j \neq i} \left(Q_j(\vec{b}) - \frac{z}{A} \int d^2b Q_j(b) \right) \tag{A11}$$

and

$$\Delta W_{inter} = Nx \sum_i \int d^2b Q_i(\vec{b}) \sum_j \left(\sum_{\rho_\beta \neq 0} Q_j(\vec{b} - \vec{\rho}_\beta) - \frac{z}{A} \int d^2b Q_j(b) \right). \tag{A12}$$

The sum between the parentheses in the above expression for ΔW_{inter} is directly related to the correlation pair function of the solid [19].

Application to SiO_2

Equations (A11) and (A12) are straightforwardly generalized as

$$\Delta W_{intra} = N_{SiO_2} x \sum_{atom=1}^{3} \sum_{i=1}^{n_{atom}} \int d^2b Q_i^{atom}(\vec{b}) \times \sum_{j \neq i}^{n_{atom}} \left(Q_j^{atom}(\vec{b}) - \frac{z}{A} \int d^2b Q_j^{atom}(b) \right), \tag{A13}$$

where $atom = 1$ means Si and 2 and 3 means oxygen atoms. n_{atom} is the number of electrons for each atom (14 for Si and 8 for O). Here z is taken as one (one molecule) and $A = N_{SiO_2}^{-2/3}$.

For the interatomic bunching within a SiO_2 molecule, the bunching reads

$$\Delta W_{inter} = N_{SiO_2} x \sum_{atom=1}^{3} \sum_{i=1}^{n_{atom}} \int d^2b Q_i^{atom}(\vec{b}) \times \sum_{atom' \neq atom} \sum_{j=1}^{n_{atom'}} \left(\sum_{\vec{\rho}_\beta^{atom,atom'} \neq 0} Q_j^{atom'} \times (\vec{b} - \vec{\rho}_\beta^{atom,atom'}) - \frac{z}{A} \int d^2b Q_j^{atom'}(b) \right). \tag{A14}$$

Finally the sum $\Sigma_{\vec{\rho}_\beta^{atom,atom'} \neq 0} Q_j^{atom'}(\vec{b} - \vec{\rho}_\beta^{atom,atom'})$ was averaged out over all directions considering interatomic distances $d_{Si\text{-}O} = 1.66$ Å and $d_{O\text{-}O} = 2.60$ Å.

The dominating term is by far the intra-atomic bunching ΔW_{intra} (more than 90% of the correction). The interatomic bunching is very small (and also negative), as was already observed in some solids using the full pair correlation function [19].

[1] M. Famá, J.C. Eckardt, G.H. Lantschner, and N.R. Arista, Phys. Rev. Lett. **85**, 4486 (2000).

[2] D.G. Arbó, M.S. Gravielle, J.E. Miraglia, J.C. Eckardt, G.H. Lantschner, M. Famá, and N.R. Arista, Phys. Rev. A **65**, 042901 (2002).

[3] N. Bohr, K. Dan. Vidensk. Selsk. Mat. Fys. Medd. **18**, 8 (1948).

[4] I. Abril, R. Garcia-Molina, N.R. Arista, and C.F. Sanz, Nucl. Instrum. Methods Phys. Res. B **190**, 89 (2000).

[5] W.K. Chu, Phys. Rev. A **13**, 2057 (1976).

[6] A. Valenzuela and J.C. Eckardt, Rev. Sci. Instrum. **42**, 127 (1971).

[7] P. Bauer, W. Rössler, and P. Mertens, Nucl. Instrum. Methods Phys. Res. B **69**, 46 (1992).

[8] J.C. Eckardt and G.H. Lantschner, Thin Solid Films **249**, 11 (1994).

[9] P. Mertens, Nucl. Instrum. Methods Phys. Res. B **27**, 315 (1987).

[10] J.F. Ziegler, J.P. Biersack, and U. Littmark, *The Stopping and Range of Ions in Solids* (Pergamon Press, New York, 1985); SRIM program: http://www.SRIM.org

[11] J.S. Williams and W. Möller, Nucl. Instrum. Methods **157**, 213 (1978).

[12] W.K. Chu, J.W. Mayer, and M.-A. Nicolet, *Backscattering Spectrometry* (Academic Press, New York, 1978), Chap. 4.

[13] F. Besenbacher, J.U. Andersen, and E. Bonderup, Nucl. Instrum. Methods **168**, 1 (1980).

[14] Y. Kido, Nucl. Instrum. Methods Phys. Res. B **24/25**, 347 (1987).

[15] M.S. Livingston and H.A. Bethe, Rev. Mod. Phys. **9**, 245 (1973).

[16] U. Fano, Annu. Rev. Nucl. Sci. **13**, 1 (1963).

[17] E. Bonderup and P. Hvelplund, Phys. Rev. A **4**, 562 (1971).

[18] P. Sigmund, K. Dan. Vidensk. Selsk. Mat. Fys. Medd. **40**, 5 (1978).

[19] P. Sigmund, in *Interaction of Charged Particles with Solids and Surfaces*, edited by A. Gras-Martí, H.M. Urbassek, N.R. Arista, and F. Flores (Plenum, New York, 1991), p. 73.

[20] P.L. Grande and G. Schiwietz, Phys. Rev. A **58**, 3796 (1998); G. Schiwietz and P.L. Grande, Nucl. Instrum. Methods Phys. Res. B **153**, 1 (1999).